J Neurosurg 103:146–155, 2005

Hemodynamic changes due to stent placement in bifurcating intracranial aneurysms

GÁDOR CANTÓN, PH.D., DAVID I. LEVY, M.D., AND JUAN C. LASHERAS, PH.D.

Department of Mechanical and Aerospace Engineering, University of California, San Diego; Department of Neurosurgery, Kaiser Permanente Medical Center, San Diego, California

Object. The aim of this study was to measure changes in intraaneurysm flow dynamics and mechanical stresses resulting from the placement of Neuroform stents in bifurcating intracranial aneurysm models.

Methods. A digital particle image velocimetry (DPIV) system was used to measure the pulsatile velocity and shear stress fields within the aneurysm and at the aneurysm neck–parent artery interface. The DPIV system provides an instantaneous two-dimensional measurement of the temporal and spatial variations of the velocity vector field of the flow inside the aneurysm pouch and the parent vessel, providing information on both the temporal and spatial variations of the velocity field during the entire cardiac cycle. The corresponding shear stress field was then computed from the velocity field data. A flexible silicone model of bifurcating intracranial aneurysms was used. Two Neuroform stents with a 60- to 65-μm strut thickness and an 11% metal/artery ratio were placed in a Y-configuration, and measurements were obtained after placing the stents.

Conclusions. Two three-dimensional vortices of different strengths persisted within the aneurysm during the entire cardiac cycle. The peak velocity and strength of these vortices were reduced after placing the two bifurcating stents. The effect of placing the Neuroform stent across the neck of a bifurcating intracranial aneurysm was shown to reduce the magnitude of the velocity of the jet entering the sac by as much as 11%. Nevertheless, the effect of the stents was particularly noticeable at the end of the cardiac cycle, when the residual vorticity and shear stresses inside the sac were decreased by more than 40%.

KEY WORDS • bifurcating aneurysm • intracranial aneurysm • wall stress • hemodynamics • stent

BALLOON-EXPANDABLE coronary stents have been placed to support coil embolization in humans[9] for several years. This stent-assisted technique has facilitated the treatment of broad-necked aneurysms that otherwise would not have been treated with endovascular therapy. There are several advantages in using stents in conjunction with coils. The presence of the stent reduces the risk of coil protrusion into the parent vessel. As the inflow is disturbed, the residence time of the platelets is increased; therefore the possibility of platelet adhesion on the vessel wall or coils is also increased,[3] thus promoting aneurysm thrombosis. Finally, the stent provides a physical matrix for possible endothelial growth, potentially facilitating the remodeling of both the aneurysm neck and the parent vessel.[20]

Preliminary clinical experience and experimental study data have demonstrated that simply crossing the aneurysm with a stent (or stents) may partially redirect blood flow away from the aneurysm sac, in some cases promoting a reduction in the intraaneurysm flow velocity and the formation of a stable thrombus.[4,11,13,14,20,21]

There are very few case reports featuring successful aneurysm occlusion through the use of one stent. Lanzino, et al.,[13] reported on four aneurysm cases treated with only one stent, although occlusion was not achieved. Aneurysm thrombosis may be accelerated using more than one stent reducing the permeability. In fact, there are some reported cases[2,4] in which the reduction of inflow due to the double placement of stents was sufficient to accelerate the formation of a thrombus within the aneurysm, thus providing a potentially viable new treatment. Note, however, that the use of the stents was limited by the fact that they were de-

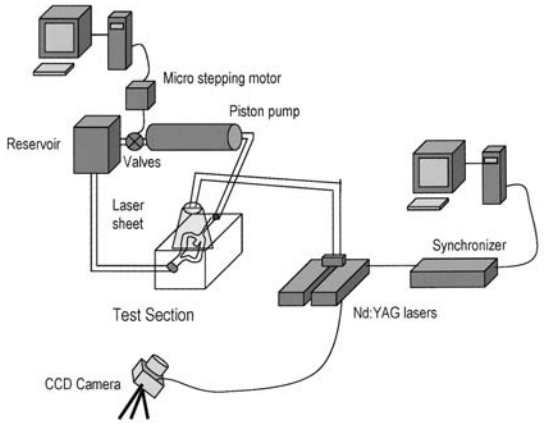

FIG. 1. Schematic of experimental setup. CCD = charge-coupled device.

Abbreviations used in this paper: BA = basilar artery; DPIV = digital particle image velocimetry; PCA = posterior cerebral artery; 2D = two-dimensional; 3D = three-dimensional.

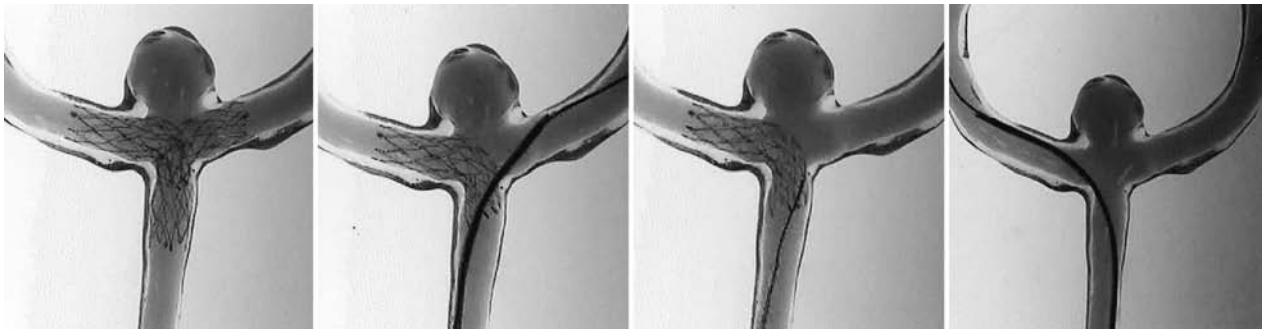

FIG. 2. Photographs depicting sequential placement of the stents in a Y-configuration across the aneurysm neck.

vised for the treatment of coronary arteries, and therefore their design prevented safe navigation through the tortuous cerebral vasculature.[17] The Neuroform stent (Boston Scientific/Neurovascular, Fremont, CA) is a flexible, self-expanding, microcatheter-delivered nitinol stent specifically designed for the treatment of cerebral aneurysms.[10] Fiorella, et al.,[5] reported on the treatment of 22 aneurysms with Neuroform stents. In four cases the aneurysm was treated using only the Neuroform stents; in one of these four cases these authors performed the double-placement technique to remodel a dissecting aneurysm.

The aim of our study was to quantify the effect of the stents by accurately measuring the changes in the hemodynamic forces acting on a bifurcating aneurysm model (basilar tip configuration) after the placement of two stents with a Y-configuration. For this purpose, a DPIV technique was used to measure the pulsatile velocity field at the entrance and inside the sac of a silicone model of a basilar tip aneurysm with a realistic prototypical shape. Measurements of velocity, vorticity, and shear stresses were obtained in a control model and compared with those obtained after placing a Y-configuration stent.

Materials and Methods

Figure 1 schematically shows the layout of the experimental setup and measurement system. The aneurysm model was made from silicone in an attempt to reproduce the compliance of the arterial wall.[12] A cadaveric cast was used to reproduce the BA (4 mm in diameter) and a 10-mm aneurysm was placed at its apex. The dimensions, curvature, and shape of the parent vessel resembled those corresponding to the BA. Note that the vessels at the bifurcation were modified slightly to situate them in the same plane as the parent artery. The angle of the PCA takeoff was kept but flattened to two dimensions to allow the laser sheet to illuminate the entire area.

To analyze the effect of placing stents, two flexible Neuroform stents were placed across the aneurysm neck in a Y-configuration. The first stent was placed distally in the PCA and proximally in the BA. The second stent was threaded through the filaments of the first and placed in the other PCA in a similar fashion (Fig. 2).

The aneurysm model was perfused with a mixture of deionized water and ethylene glycol in a volume ratio of approximately 60:40. The fluid viscosity was 2.5 cp (at room temperature) and had a density of 1.03 kg/dm^3. The fluid was seeded by lycopodium powder (Carolina Biological Supply Company, Burlington, NC) with a mean diameter between 1 and 10 μm. To avoid distortion of the visualized flow by refraction, the model was placed in a transparent box filled with the same perfusion fluid.

A pulsatile flow corresponding to the flow through the carotid artery was supplied to the model by a pulsatile pump (UHDC flow system; Sidac Engineering, Toronto, ON, Canada). Figure 3 shows the waveform input from the pump into the aneurysm model. The peak volume rate selected for this study was 360 ml/minute. The period of the pulsatile flow was 0.83 seconds, corresponding to a cardiac rate of 72 bpm.

To quantify the instantaneous 3D velocity field inside the aneurysm model, DPIV (TSI, Inc., St. Paul, MN) was used. The system was composed of two Nd:YAG lasers, a synchronizer, a charge-cou-

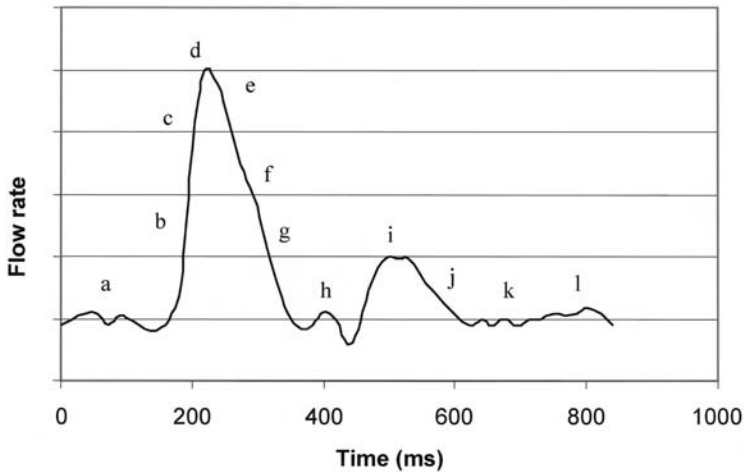

FIG. 3. Graph demonstrating waveform corresponding to the flow in the carotid artery. ms = msec.

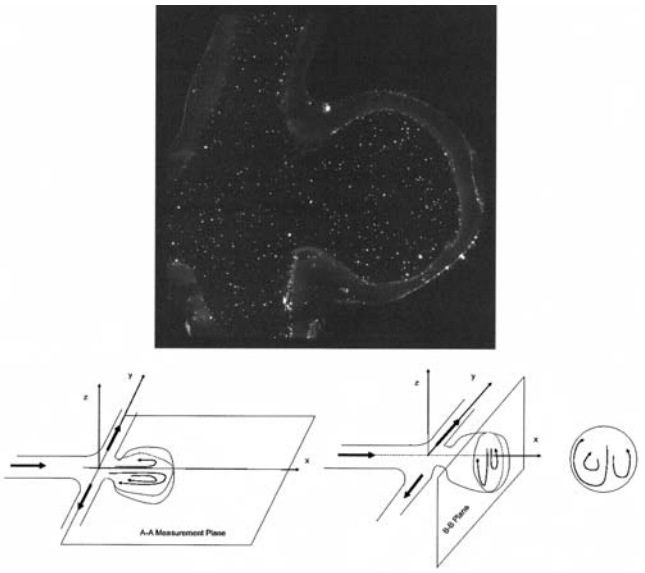

FIG. 4. *Upper:* Cross-cut plane illuminated by the planar laser sheet. The speckles are the light-scattering of lycopodium particles used for the DPIV measurements. *Lower:* Schematics depicting the 3D flow to be expected in the cross-cut of the basilar tip aneurysm where the measurements were obtained *(left)*, and a plane normal to the direction of the jet entering the aneurysm sac *(right)*.

pled device camera, and a personal computer. The pulsed lasers provided a laser sheet that illuminates the small tracer particles added to the flowing fluid. The firing of the two pulsed lasers was synchronized with the image acquisition. Two consecutive images corresponding to the firing of each laser, 0.4 msec apart, were captured when the camera was triggered by the synchronizer, thus recording the light scattered by the tracer particles.

The fundamental principle of DPIV is to measure the particle displacements Dx, Dy from statistical correlations of each pair of images. These displacements must be small enough that Dx/Dt is a good approximation of the x-velocity; that is, the trajectory of the particle in this very short time interval must be nearly straight and the speed along the trajectory nearly constant. Therefore, Dt, the time between the two pulses of the lasers, is chosen to be small compared with the relevant flow times of the experiment. Each Nd:YAG laser was pulsed at 15 Hz. Thus, for each cardiac cycle, 12 to 13 pairs of images at the times indicated in Fig. 3 (a to l on the flow waveform) were obtained. The velocity field is then computed using the appropriate software (Insight; TSI, Inc.), cross-correlating the two images. The cross-correlation function is computed via performing 2D fast-Fourier transforms. Once the velocity field is computed, the data are transferred to Tecplot software (Amtec Engineering, Inc., Bellevue, WA) to compute other flow quantities such as the vorticity and the shear forces.

Results

Measurements of velocity, vorticity, and shear stress in the aneurysm with a stent were compared with the corresponding measurements in the control. To conduct a systematic comparison, we selected the measurement of the velocity field in an axial plane running along the centerline of the basilar tip aneurysm and dissecting the aneurysm sac at a midpoint (Fig. 4). The two PCAs were also contained in this plane.

Control Aneurysm

Measurements of the velocity field in the control aneurysm without a stent, performed at 12 sequential stages of the cardiac cycle, are shown in Fig. 5. The *arrows* represent the measured velocities and indicate both their magnitude and direction. These instantaneous velocity measurements were conducted at 1/15 of 1 second apart from each other and correspond to the times along the cardiac cycle marked a through l in Fig. 3.

At peak systole (Fig. 5d) a very strong jet is seen entering the aneurysm sac. This jet is then projected onto the aneurysm fundus. The instantaneous streamlines corresponding to the flow at peak systole are shown in Fig. 6. These streamlines clearly show that at the impact point (stagnation point), the jet bifurcates into a very strong clockwise-rotating vortical flow engulfing most of the central and lower portions of the sac, and a much weaker counterclockwise-rotating vortical motion confined to the upper section of the sac. The *arrow* labeled SP marks the location of the stagnation point, that is, the wall impingement point. During one diastole, these two vortical motions persist. In particular, we were able to determine from time frames f to l that the stronger vortex, although decaying in strength due to viscous dissipation, retains its coherency, and the clockwise rotation of the flow persists until the end of the cardiac cycle. The persistence of the rotational motion is a direct consequence of the large rotational inertia generated by the splitting jet on impact with the fundus, a condition typical of basilar tip aneurysms in which the incoming blood flow is directed straight into the aneurysm sac. The asymmetric form of the flow in the sac is simply a consequence of the small geometric asymmetries, which are also typical of this arterial configuration. In fact, the asymmetric nature of the flow is a characteristic to be expected as the norm rather than as an exception.[6]

It is important to mention that the velocity vector fields shown in Fig. 5 were measured only in the axial plane (A-A plane in Fig. 4) and that the flow motion in the aneurysm sac is 3D and not confined to this plane. Although not included here, measurements of the velocity field in a B-B plane perpendicular to the jet entering the sac show that the blood flow also rotates in the azimuthal direction in the normal plane, as schematically shown in Fig. 4.

The 2D component of the vorticity field ($\omega_z = 0.5[\partial u/\partial y - \partial v/\partial x]$), corresponding to the measurements shown in Fig. 5, is featured in Fig. 7. The isocontours of the vorticity vector are indicated by varying intensities of red (counterclockwise vorticity) and blue (clockwise vorticity). These measurements show that vorticity reaches a maximal value at the peak systole and that these large values are associated with the presence of the strong jet entering the sac. It is also important to point out that never throughout the cardiac cycle does the flow in the sac reach stasis or the vorticity become negligible.

The corresponding 2D component of the strain rate ($\epsilon_z = 0.5[\partial u/\partial y + \partial v/\partial x]$) fields are shown in Fig. 8. The flow shear stresses are directly proportional to these values, with the constant of proportionality being the viscosity ($\tau_z = \mu\epsilon_z$, where μ is the flow viscosity). These stress fields show several important features. First, at peak systole (Fig. 8d), one sees a region of very large gradients of wall shear stresses located at the stagnation point marked by SP. This point separates regions of large gradients in the magnitude but, most importantly, in reversing sense in the direction of the wall shear stresses (τ_ω). Second, these measurements also show that due to the persistent vortical motion, the wall shear

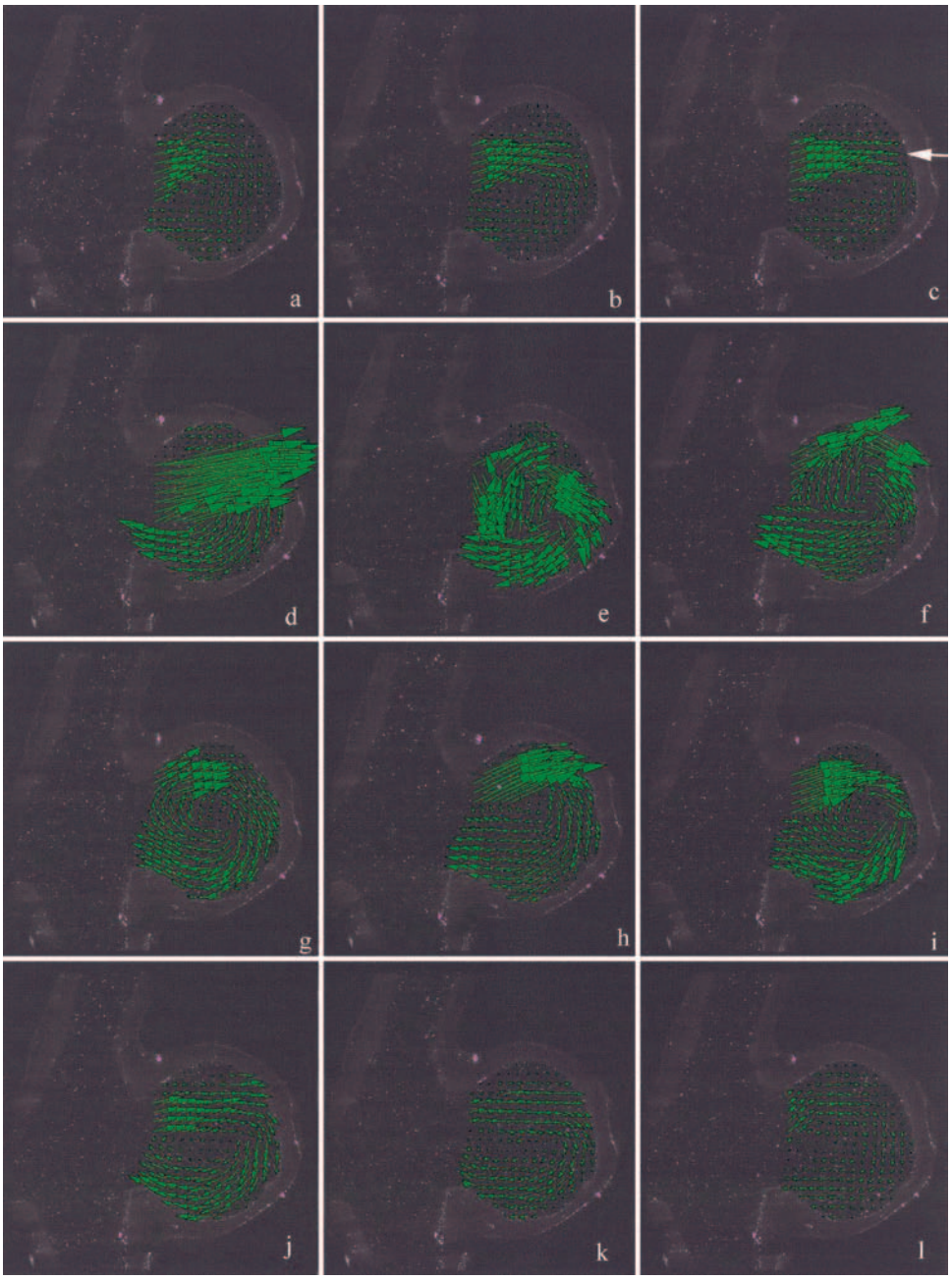

FIG. 5. Images demonstrating the velocity field corresponding to the untreated bifurcating aneurysm model. *Arrow* indicates the position of the stagnation point, where the flow impinges on the wall and bifurcates.

stresses at the end of the cardiac cycle never decay to zero anywhere on the walls of the aneurysm sac.

In summary, measurements in the control aneurysm showed that the flow inside the sac is composed of a complex, 3D motion dominated by the presence of a bifurcating jet, which leads to the formation of two vortices of uneven strength. Due to the strong centrifugal inertia resulting from this vortical motion, the rotational flow inside the aneurysm never stops, not even during the resting period of the cardiac cycle. Furthermore, regions of large gradients of wall shear stresses and spikes of high pressure are created at the location where the jet impinges on the wall (SP).

Aneurysm With Stent

We conducted an identical set of measurements in the aneurysm with a stent while being perfused with the same waveform as in the control aneurysm described previously. The sequential measurements of the velocity field in the axial plane are featured in Fig. 9. The labeling of these frames corresponds to the identical time frames in the cardiac cycle as in the control (Fig. 5).

Our measurements showed that in a qualitative sense the flow retains some of the characteristics as those discussed for the control. Nevertheless, it is apparent that both the

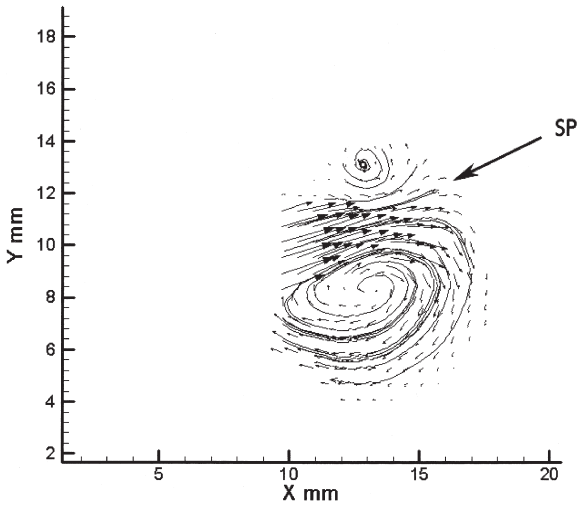

FIG. 6. Graphic representation of instantaneous streamlines showing the presence of two counter-rotating vortices inside the aneurysm pouch. *Arrow* indicates the location of the stagnation point (SP).

strength of the jet entering the sac at peak systole and the strength of the resulting vortices within the sac were somewhat modified by the stents. An increased loss of symmetry was also noted whereby the weak counterclockwise-rotating upper vortex was virtually absent.

To quantify changes resulting from the placement of the stents, we compared the values of velocity, vorticity, and shear stresses at two representative stages along the cardiac cycle: peak systole (d in Fig. 3) and the end of the cardiac cycle (l in Fig. 3).

Figure 10 shows a comparison of the magnitude of the velocity field in both the control and the treated aneurysms at peak systole. Note that in the case treated with a stent, flow was also dominated by the presence of a jet, which seemed to be deflected slightly upward and somewhat weaker. In both cases, upon impingement of the fundus, the jet bifurcates into two vortices of uneven strengths. Table 1 features a comparison of the mean maximal values of the velocity, vorticity, and strain rate measured at peak systole in the control aneurysm and in the lesion treated with stents. These mean values were calculated over five cycles, and one should note that there was a sizeable cycle-to-cycle variation in these measurements. In fact, these measurements

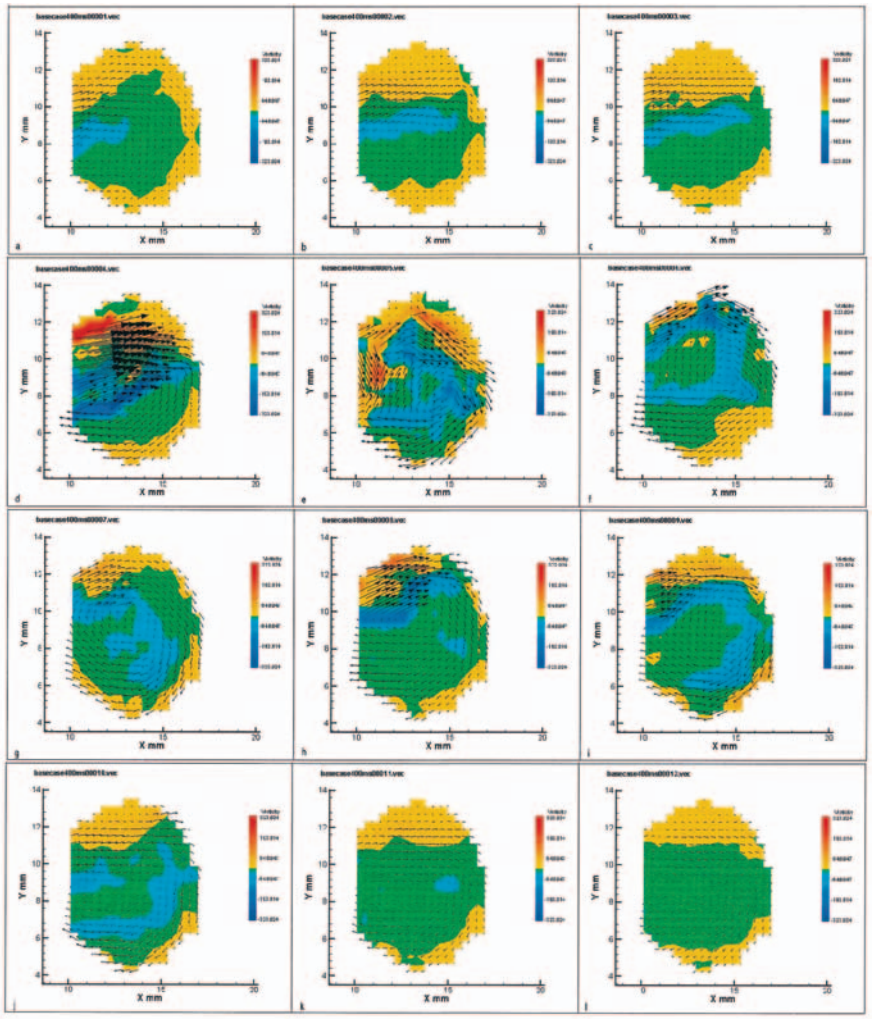

FIG. 7. Images depicting the vorticity field inside a bifurcating aneurysm measured throughout the entire cardiac cycle.

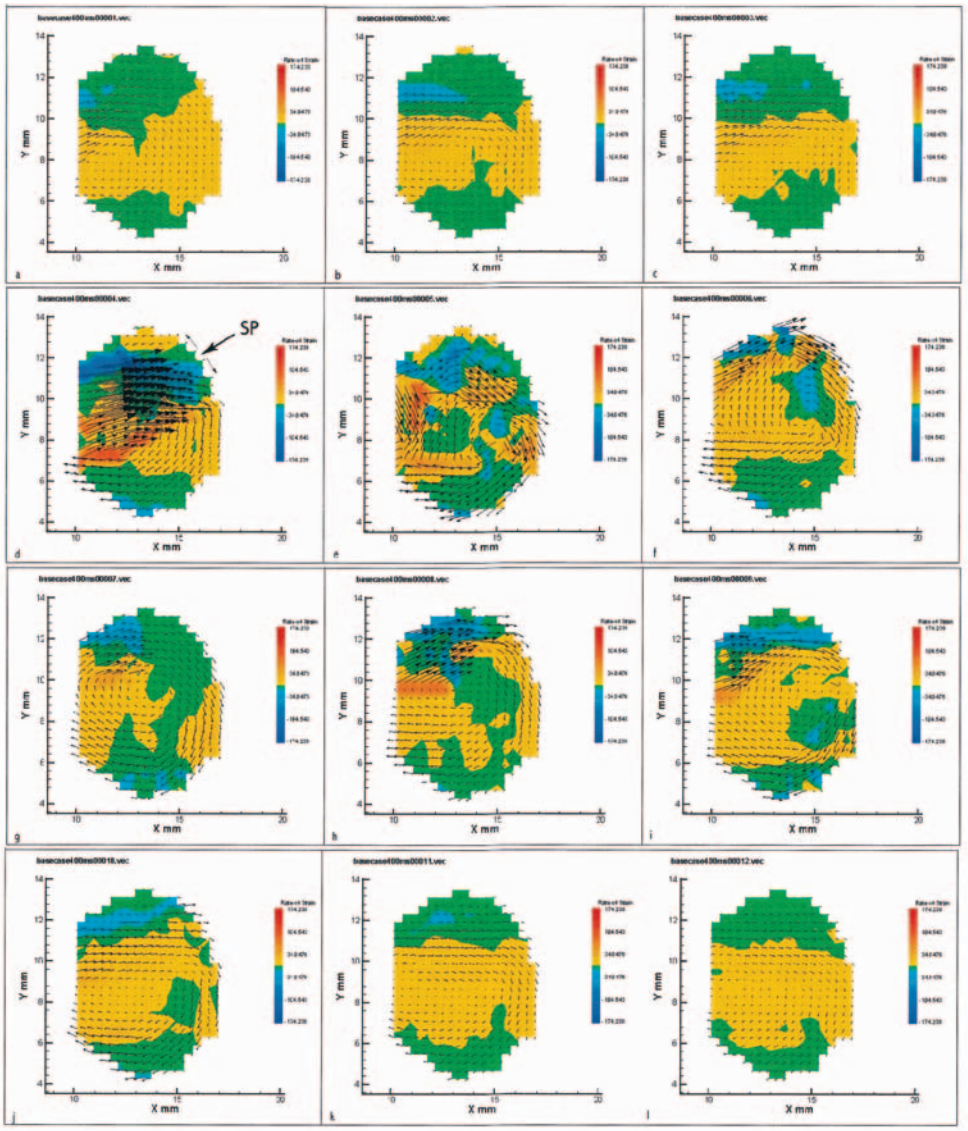

FIG. 8. Images depicting the shear rate field inside a bifurcating aneurysm measured throughout a complete cardiac cycle.

showed a net reduction of 11% in the maximal value of the velocity magnitude, a 5.8% reduction in the maximal vorticity value, and a 9% reduction in the maximal value of the shear stress, when the aneurysm neck was crossed with the two stents in a Y-configuration.

A comparison of the measured velocity magnitude at the end of the cardiac cycle (l in Fig. 3) in both the aneurysm with the stents and the control is featured in Fig. 11. Although qualitatively speaking the two flows are very similar, one can see that the remnant rotational motion is much weaker in the aneurysm with the stents. Table 1 shows a comparison of the mean maximal values of the velocity magnitude, vorticity, and shear stress measured at the end of the cardiac cycle, in both cases. Note that in the aneurysm with the stents, vorticity was nearly depleted, having a value 58% of that in the control, and the corresponding maximal shear stress was also drastically reduced to a value 59% of that in the control.

TABLE 1

Comparison of the maximal mean values of the velocity, vorticity, and strain rate fields at both peak systole and peak diastole in the control and the treated aneurysms

Time & Case	Velocity Magnitude (m/sec)	Vorticity (1/sec)	Strain Rate (1/sec)
systole			
control	0.35 ± 0.18	206.68 ± 92.34	90.56 ± 43.54
stent	0.32 ± 0.07	195.25 ± 74.26	81.91 ± 34.20
diastole			
control	0.04 ± 0.01	21.81 ± 6.04	10.75 ± 3.46
stent	0.02 ± 0.002	6.90 ± 1.50	3.17 ± 0.70

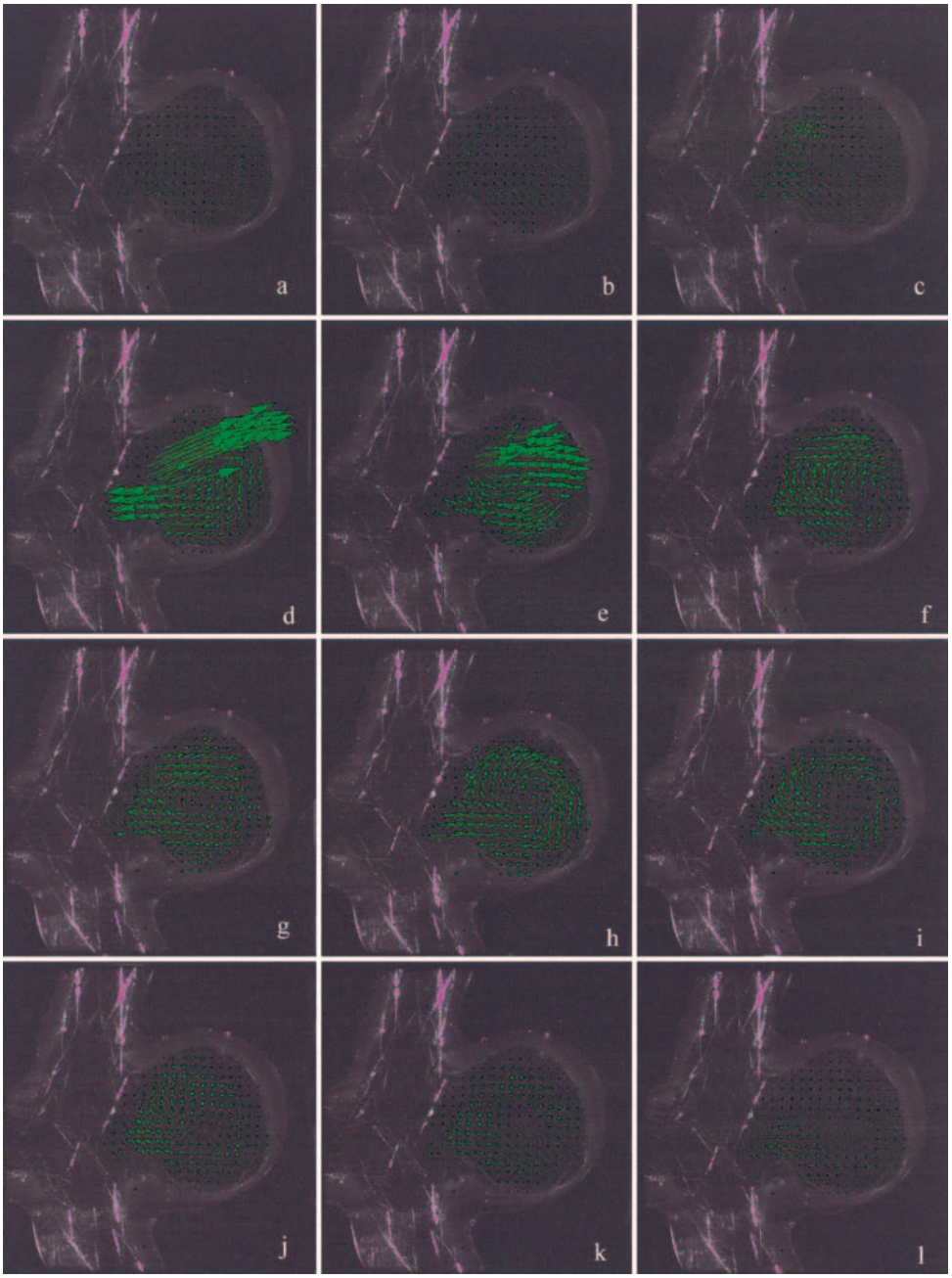

FIG. 9. Images depicting the velocity field, throughout a complete cardiac cycle, in the aneurysm dome after placing the stents across the aneurysm neck.

Discussion

Hemodynamic Changes Due to Stent Placement

It has been argued that intraaneurysm stasis may result from resistance to flow into the aneurysm through the stent mesh together with a low-pressure gradient between the parent artery and the aneurysm.[1] To quantify the effect of placing stents, we compared the mean magnitude of the velocity, vorticity, and shear stress, values measured both before and after placing the stents for two representative stages of the cardiac cycle—peak systole and the end of the cycle. The small decrease in the mean velocity of the jet entering the aneurysm was due to the fact that the pressure drop across the stent mesh was very small; the porosity of the combined stents was still very large (11% metal/artery ratio with a 4-mm Neuroform stent). This very small pressure drop caused small changes (11%) in the mean velocity of the jet.

The wire mesh formed by the stent filaments produced a small-scale (high-frequency) turbulence in the aneurysm sac. This small-scale turbulence in the high-frequency range contributed to an enhanced dissipation rate due to viscosity. This effect was responsible for the very rapid decay in rotational motion in the aneurysm sac with the stents and for the

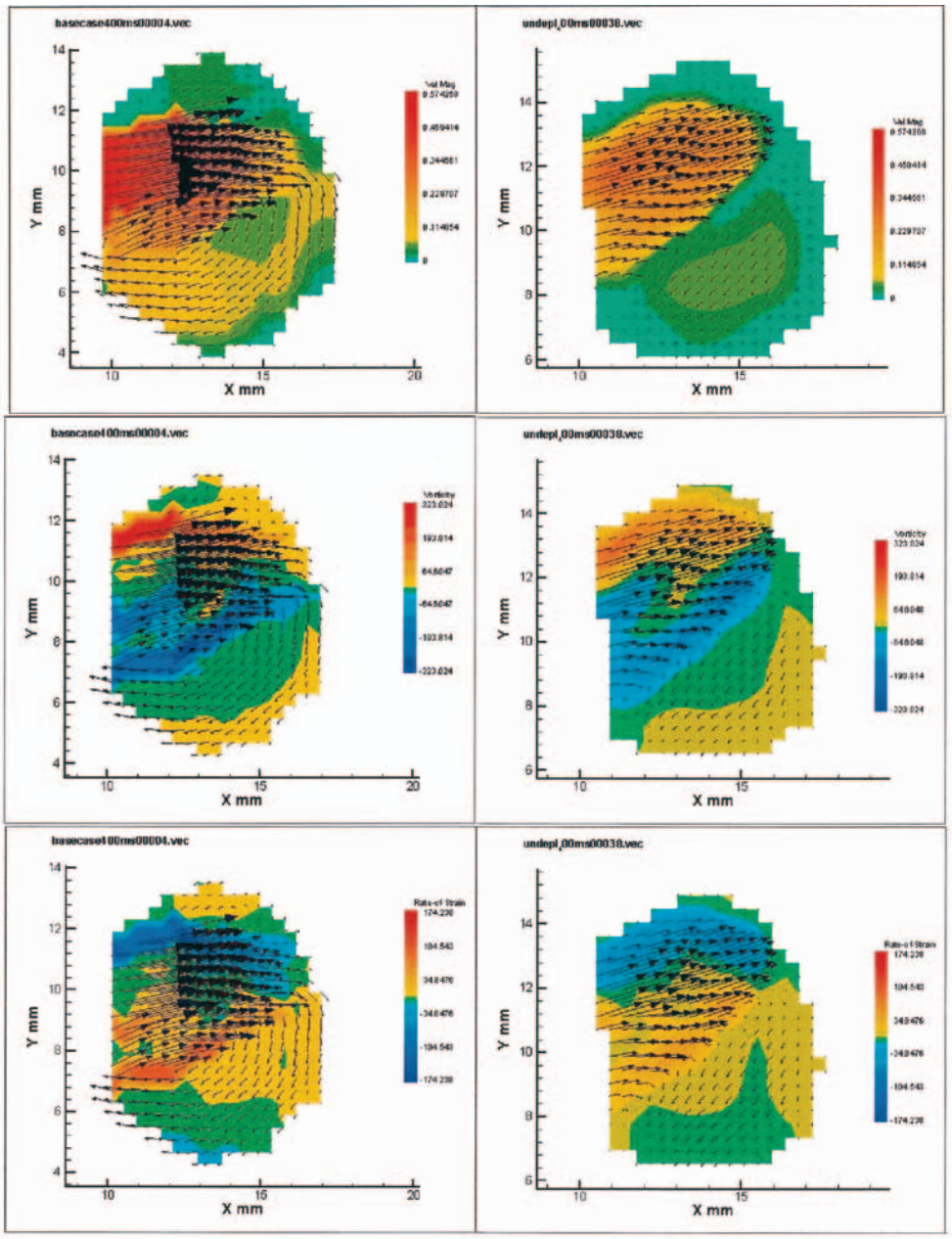

FIG. 10. Images demonstrating the magnitude of the velocity *(upper)*, vorticity *(center)*, and shear strain *(lower)* fields at peak systole. Plots on the *left* correspond to the control, whereas those on the *right* correspond to the aneurysm with the stents.

almost static condition by the end of the cardiac cycle. Similar results demonstrating enhanced decay of the rotational motion have been reported by authors of previous studies.[1,14,21]

Limitations of The Experimental Setup

In the experiments reported here, the blood was simulated as a Newtonian fluid. This assumption was reasonable since the diameter of the intracranial arteries is large enough (> 0.1 mm) to achieve the high rate of shear needed for the blood to behave as a Newtonian fluid,[8,15] and the non-Newtonian rheology of the blood on the wall shear in these vessels has been shown to have a negligible effect.[7,16]

The aneurysm model used in this study was a representative case of a bifurcating aneurysm such as those that appear in the basilar tip or in the internal carotid artery. Although the reduction in the velocity, vorticity, and stresses reported here were specific to the particular geometry selected, the decay in these flow quantities at the end of the cardiac cycle was large enough to expect the same reduction in all types of bifurcating aneurysms.

Both aneurysms and healthy human vessels vary greatly with patient age and individual anatomy. No two aneurysms

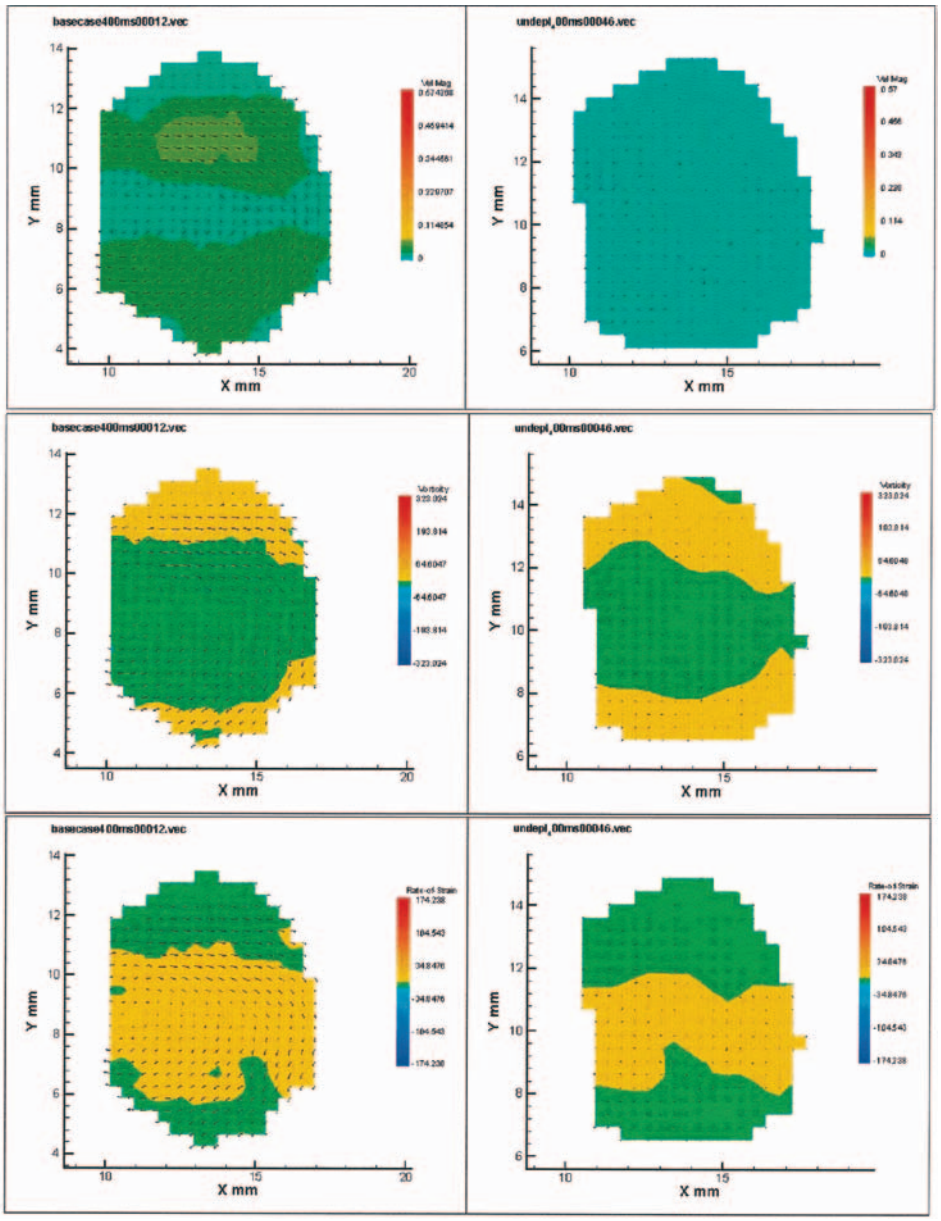

FIG. 11. Images depicting the velocity magnitude *(upper)*, vorticity *(center)*, and strain rates *(lower)* fields at the end of the cardiac cycle. *Left* images represent those in the control, whereas the ones on the *right* correspond to the aneurysm with stents.

are exactly alike in all properties, and we therefore used an approximation of the compliance of the aneurysm walls by using silicone models.[12] Our models reproduced only qualitatively the actual elastic modulus of the arterial wall. Nevertheless, it has been shown that the flow pattern does not change with the small deformations due to the elastic properties of the arterial wall.[18,19] Thus, the results presented here should be directly applicable to in vivo situations.

Conclusions

We performed a comparative study of the changes in velocity, vorticity, and shear stresses resulting from placing two Neuroform stents in a Y-configuration across the neck of a bifurcating aneurysm. We measured a small reduction in the maximal value of the wall shear stress (at peak systole) after placement of the stents. Nevertheless, our measurements showed a considerable reduction in the stresses during diastole together with an increase in the duration of time for which the wall shear stresses were very small. This large increase in the time during which shear levels are negligibly small could play a significant role in inhibiting future aneurysm growth. Although the complete answer to this question should come from clinical data, our measurements revealed an alternative therapy whose potential should be investigated further. The marked reduction in the residual rotational motion inside the aneurysm sac together with the associated large reduction in the vorticity and shear stress

inside the sac leads one to wonder if the mere use of stents, without coil packing in the sac, could provide a viable therapy for some aneurysms.

Acknowledgment

We acknowledge Peter Kim Nelson, M.D., for his insight and involvement in this project.

Disclosure

David I. Levy, M.D., is a speaker for Boston Scientific Corporation and receives financial compensation.

References

1. Aenis M, Stancampiano AP, Wakhloo AK, Lieber BB: Modeling of flow in a straight stented and nonstented side wall aneurysm model. **J Biomech Eng 119:**206–212, 1997
2. Benndorf G, Herbon U, Sollmann WP, Campi A: Treatment of a ruptured dissecting vertebral artery aneurysm with double stent placement: case report. **AJNR 22:**1844–1848, 2001
3. Byun HS, Rhee K: Intraaneurysmal flow changes affected by clip location and occlusion magnitude in a lateral aneurysm model. **Med Eng Phys 25:**581–589, 2003
4. Doerfler A, Wanke I, Egelhof T, Stolke D, Forsting M: Double-stent method: therapeutic alternative for small wide-necked aneurysm. Technical note. **J Neurosurg 100:**150–154, 2004
5. Fiorella D, Albuquerque FC, Han P, McDougall CG: Preliminary experience using the Neuroform stent for the treatment of cerebral aneurysms. **Neurosurgery 54:**6–17, 2004
6. Foutrakis GN, Yonas H, Sclabassi RJ: Saccular aneurysm formation in curved and bifurcating arteries. **AJNR 20:**1309–1317, 1999
7. Friedman MH, Bargeron CB, Duncan DD, Hutchins GM, Mark FF: Effects of arterial compliance and non-Newtonian rheology on correlations between intimal thickness and wall shear. **J Biomech Eng 114:**317–320, 1992
8. Hademenos GJ: The physics of cerebral aneurysms. **Physics Today 48:**24–30, 1995
9. Higashida RT, Smith W, Gress D, Urwin R, Dowd CF, Balousek PA, et al: Intravascular stent and endovascular coil placement for a ruptured fusiform aneurysm of the basilar artery. Case report and review of the literature. **J Neurosurg 87:**944–949, 1997
10. Howington JU, Hanel RA, Harrigan MR, Levy EI, Guterman LR, Hopkins LN: The Neuroform stent, the first microcatheter-delivered stent for use in the intracranial circulation. **Neurosurgery 54:** 2–5, 2004
11. Imbesi SG, Kerber CW: Analysis of slipstream flow in a wide-necked basilar artery aneurysm: evaluation of potential treatment regimes. **AJNR 22:**721–724, 2001
12. Kerber CW, Heilman CB, Zanetti PH: Transparent elastic arterial models. I: A brief technical note. **Biorheology 26:**1041–1049, 1989
13. Lanzino G, Wakhloo AK, Fessler RD, Hartney ML, Guterman LR, Hopkins LN: Efficacy and current limitations of intravascular stents for intracranial internal carotid, vertebral, and basilar artery aneurysms. **J Neurosurg 91:**538–546, 1999
14. Lieber BB, Stancampiano AP, Wakhloo AK: Alteration of hemodynamics in aneurysm models by stenting: influence of stent porosity. **Ann Biomed Eng 25:**460–469, 1997
15. McDonald DA: **Blood flow in arteries, ed 2.** London: Edward Arnold, 1974
16. Perktold K, Peter RO, Resch M: Pulsatile non-Newtonian blood flow simulation through a bifurcation with an aneurysm. **Biorheology 26:**1011–1030, 1989
17. Prendergast PJ, Lally C, Daly S, Reid AJ, Lee TC, Quinn D, et al: Analysis of prolapse in cardiovascular stents: a constitutive equation for vascular tissue and finite-element modelling. **J Biomech Eng 125:**692–699, 2003
18. Steiger HJ, Poll A, Liepsch D, Reulen HJ: Haemodynamic stress in lateral saccular aneurysms. An experimental study. **Acta Neurochir 86:**98–105, 1987
19. Steiger HJ, Poll A, Liepsch DW, Reulen HJ: Haemodynamic stress in terminal aneurysms. **Acta Neurochir 93:**18–23, 1988
20. Wakhloo AK, Lanzino G, Lieber BB, Hopkins LN: Stents for intracranial aneurysms: the beginning of a new endovascular era? **Neurosurgery 43:**377–379, 1998
21. Yu SCM, Zhao JB: A steady flow analysis on the stented and nonstented sidewall aneurysm models. **Med Eng Phys 21:**133–141, 1999

Manuscript received April 13, 2004.
Accepted in final form October 25, 2004.

Address reprint requests to: David I. Levy, M.D., University of California, San Diego, Department of Mechanical and Aerospace Engineering, 9500 Gilman Drive, MC 0411, La Jolla, California 92093-0411. email: sdlev@yahoo.com.